HIGHLIGHTS FROM THE HADES EXPERIMENT*

Szymon Harabasz

for the HADES Collaboration

Technische Universität Darmstadt, Germany

Received 1 August 2022, accepted 8 September 2022, published online 14 December 2022

In these proceedings, an overview of recent results from the HADES experiment will be given, including electromagnetic probes, hadron anisotropy, and resonance production. References to strangeness results are also provided.

DOI:10.5506/APhysPolBSupp.16.1-A5

1. Introduction

The High Acceptance DiElectron Spectrometer (HADES) is a fixed-target multipurpose particle detector system located at the heavy-ion research facility in Darmstadt, Germany. The SIS18 provides a beam from protons to the heaviest ions with maximum beam energies of 4.5 GeV and 1–2 A GeV, respectively, and secondary pion beams.

The available beams are utilized to realize the two-fold physics program. Heavy-ion collisions (HICs), whose energy translates to $\sqrt{s_{NN}} = 2$–3 GeV, allow to study properties of QCD matter (such as constraining its equation-of-state) at moderate temperatures and the highest net-baryon densities studied currently in the world. Similar conditions are expected to occur in neutron star mergers.

Pion and proton beams serve for reference measurements and for studying the electromagnetic structure of baryons and hyperons.

This contribution focuses on results from the most recent data taking campaigns: Au+Au at $\sqrt{s_{NN}} = 2.42$ GeV in April 2012, Ag+Ag at $\sqrt{s_{NN}} = 2.55$ GeV and $\sqrt{s_{NN}} = 2.42$ GeV in March 2019, as well as $p + p$ at $\sqrt{s} = 3.46$ GeV and $\sqrt{s} = 2.55$ GeV in February 2022.

* Presented at the 29$^{\text{th}}$ International Conference on Ultrarelativistic Nucleus–Nucleus Collisions: Quark Matter 2022, Kraków, Poland, 4–10 April, 2022.

2. Detector setup

As shown in Fig. 1, HADES consists of six identical sectors, each covering almost 60° of the azimuthal angle. It has an acceptance covering more than one unit around mid-rapidity. Particle tracking is provided by four sets of Multiwire Drift Chambers (MDCs), two located in front and two behind the region of the magnetic field generated by superconducting coils. Particle identification is performed by time-of-flight detectors: Resistive Plate Chambers (RPC) closer to the beam axis and plastic scintillators (TOF) at larger polar angles. Identification of e^+/e^- is done with a hadron-blind Ring Imaging Cherenkov (RICH) detector and supported by an electromagnetic calorimeter, which also detects photons.

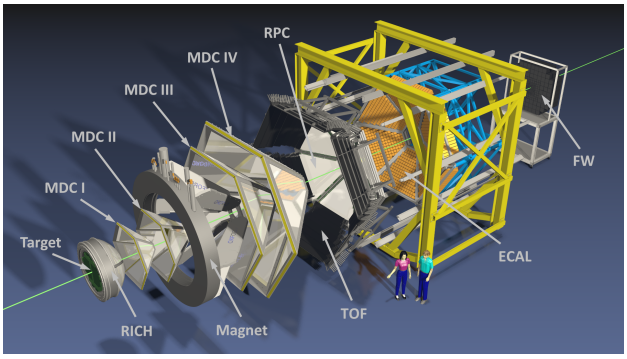

Fig. 1. A 3D scheme of the HADES detector system as used in the March 2019 Ag+Ag data taking, stretched along the beam axis direction for better visibility.

RICH has been upgraded recently in cooperation with the CBM experiment by replacing an MWPC-based photon detector with an array of photomultiplier tubes for higher detection efficiency, and close pair rejection.

In heavy-ion runs, Forward Wall (FW) — an array of plastic scintillators located 7 m behind the HADES setup — is used to determine event centrality and reaction plane. In the February 2022 $p+p$ run, the forward region was equipped with new straw tube tracking stations and a forward RPC detector — a result of synergy between the HADES and PANDA collaborations [1].

3. Electromagnetic probes

HADES was particularly designed to be able to measure dielectrons — e^+e^- pairs originating from virtual photons. In hadronic collisions, this allows to access the electromagnetic structure of baryons and hyperons in the time-like region of the four-momentum transfer. In heavy-ion collisions, once produced, dileptons decouple from the hadronic medium and leave the interaction zone essentially undisturbed.

Dilepton spectra from Ag+Ag collisions are shown in Fig. 2 for two collision energies. To access the part of the radiation coming from the hot and dense medium, contributions from pre-equilibrium NN collisions and from hadronic decays after the freeze-out have to be subtracted. The former is approximated by appropriately scaled spectra from $p+p$ and quasi-free $n+p$ collisions measured at the same collision energy as HICs, called NN reference spectra. For $\sqrt{s_{NN}} = 2.42$ GeV Au+Au and Ag+Ag experiments, NN reference is already available [2–4]. For $\sqrt{s_{NN}} = 2.55$ GeV, a dedicated data set has been collected during the February 2022 beam time, whose analysis is ongoing.

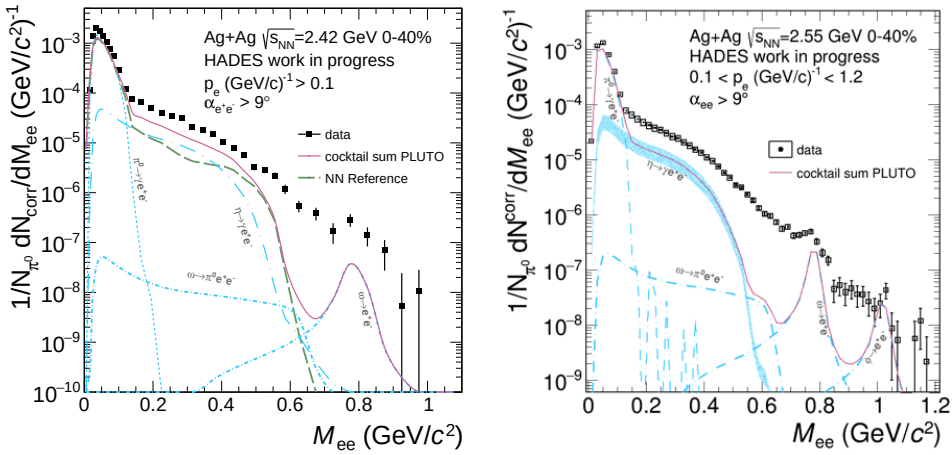

Fig. 2. (Color online) Invariant mass distributions of dileptons, measured in Ag+Ag collisions at $\sqrt{s_{NN}} = 2.42$ GeV (left) and $\sqrt{s_{NN}} = 2.55$ GeV (right), compared to the hadronic freeze-out cocktail, simulated with PLUTO [5] (each component shown as a blue line and their sum as the brown one) and to the NN reference (in the case of the lower collision energy, green line).

The freeze-out contribution is described by a cocktail of dilepton sources, constrained by the analysis of channels other than containing dileptons, simulated using PLUTO event generator [5]. For example, the π^0-Dalitz contribution is determined by the measurement of $\pi^0 \to \gamma\gamma$ with the electromagnetic calorimeter, an example of which is shown in the left panel of Fig. 3. The $\phi \to e^+e^-$ component is constrained by $\phi \to K^+K^-$, shown in the right panel of Fig. 3.

One can observe excess radiation above the NN reference and the freeze-out cocktail, which can be attributed to the radiation from the hot and dense medium. Statistics is sufficient to split further the data set and perform a multi-differential analysis, details of which, for 2.55 GeV, are discussed

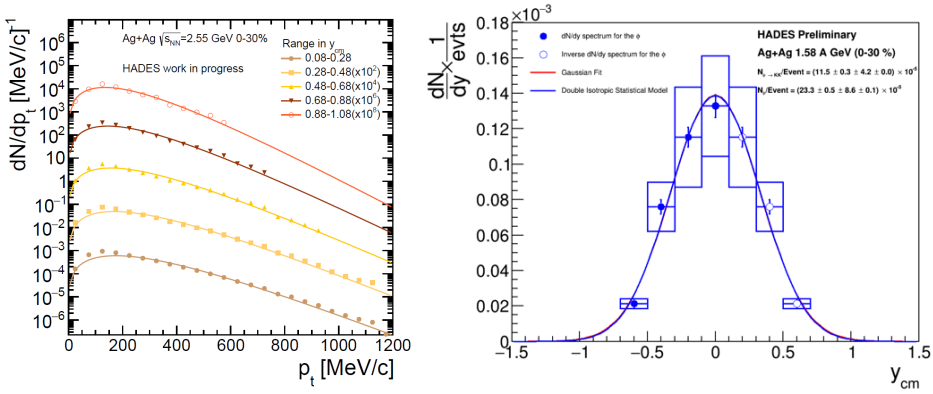

Fig. 3. Left: transverse momentum spectra in different rapidity ranges of the $\pi^0 \to \gamma\gamma$, measured with the HADES electromagnetic calorimeter. Right: rapidity distribution of the ϕ meson, measured in the K^+K^- channel.

in [6]. Another opportunity is a systematic study of the energy and system-size dependence of the excess radiation, given that in Au+Au and Ag+Ag collisions, one can select centrality classes of the comparable mean number of participating nucleons $\langle A_{\rm part}\rangle$.

4. Hadron production and collectivity

It has already been pointed out [7] that state-of-the-art hadronic transport models cannot consistently describe pion yields and momentum spectra measured by HADES. Recently, a new development has been made in the parametrization of the influence of the Coulomb field of the positively charged fireball on the pion spectra. An important tunable parameter — effective potential energy — can be translated to the size of the fireball, which is found in good agreement with values obtained in the Statistical Hadronization Model [8].

Azimuthal anisotropy coefficients $v_n = \langle\cos(n(\phi_p - \Psi_{\rm RP})\rangle$ (where ϕ_p is the azimuthal direction of particle's momentum and $\Psi_{\rm RP}$ is the reaction plane orientation) for hadrons are sensitive to the equation-of-state of the matter. Figure 4 shows an example of HADES measurements: $v_1(y_{\rm cm})$ (where $y_{\rm cm}$ is the rapidity in the center-of-mass of the colliding system) of π^+ measured in Au+Au and Ag+Ag reactions and of K^+ measured in Au+Au, compared to a set of hadronic transport calculations. For pions, the rapidity dependence of the directed flow is stronger in most calculations than observed in the experiment. In the case of kaons, no model would perfectly reproduce the rapidity dependence, while the PHSD and GiBUU with kaon potential are close.

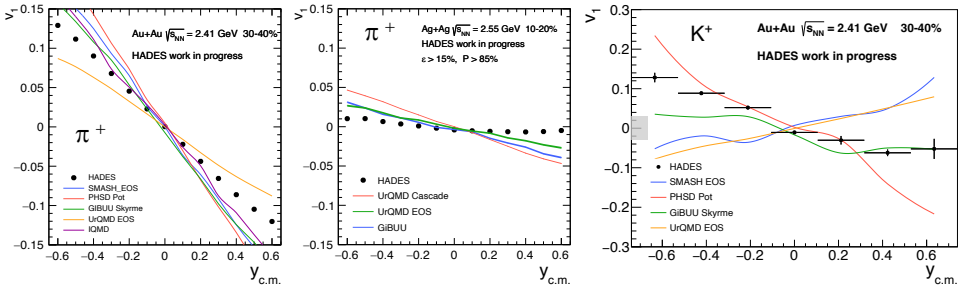

Fig. 4. Azimuthal anisotropy harmonic v_1 for π^+ measured by HADES in Au+Au at $\sqrt{s_{NN}} = 2.42$ GeV (left), Ag+Ag at $\sqrt{s_{NN}} = 2.55$ GeV (middle), and for K^+ in Au+Au at $\sqrt{s_{NN}} = 2.42$ GeV (right), compared to available transport model calculations.

Like dilepton spectra, azimuthal anisotropy observables can be studied systematically as a function of collision energy and system size.

5. The relevance of the meson cloud

In the energy range of heavy-ion collisions studied by HADES, strangeness is produced below the corresponding threshold for NN collisions. This makes the measurements particularly sensitive to medium effects.

It has been observed that in Au+Au collisions, yields of all strange particles scale with $\langle A_{\rm part}\rangle$ according to a power law with a common exponent [9]. The same observation is now made in the Ag+Ag data [10], but with the value of the exponent slightly different than in Au+Au. Since different particle species have different production thresholds in NN collisions, this observation suggests that strange quarks can be easily exchanged between hadronic states before the chemical freeze-out. Such an exchange can be facilitated by the percolation of meson clouds surrounding hard hadron cores. According to the calculation with quantum effects included, this should happen at a density equal to $1.8\rho_0$, where ρ_0 is the nuclear saturation density [11]. Such densities are easily reached in HICs at HADES energies, see *e.g.* [12].

The effect of the pion cloud is also visible in exclusive $pp \to pp\,e^+e^-$ [4] and $\pi^- p \to n\,e^+e^-$ [13] reactions. An example of the latter is presented in Fig. 5 which shows the measured dilepton invariant mass distribution and the ratio to the QED expectation (point-like hadrons). The ratio deviates strongly from unity towards higher masses, indicating the relevance of off-shell ρ mesons.

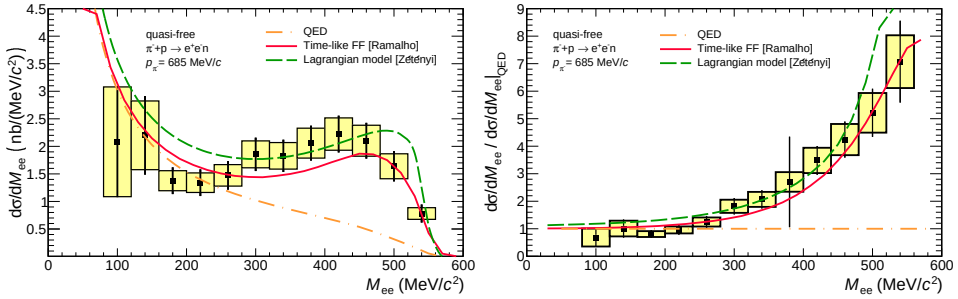

Fig. 5. Left: dilepton distribution, measured in $\pi^- p \to n\, e^+ e^-$ reactions, compared to a simple prediction assuming decays of point-like resonances (denoted "QED") and to the calculations of [14–16]. Right: ratio to the QED model.

6. Studying baryon resonances with heavy-ion data

One can study resonance properties not only in πp collisions but also by analyzing πp states in heavy-ion collisions. After a novel method of dealing with combinatorial background has been developed [17], HADES provided a rich set of high-precision data on correlated pion–proton pairs [18]. Examples shown in the left and the middle panel of Fig. 6 demonstrate the quality of the data and its usefulness in constraining the resonance description in models.

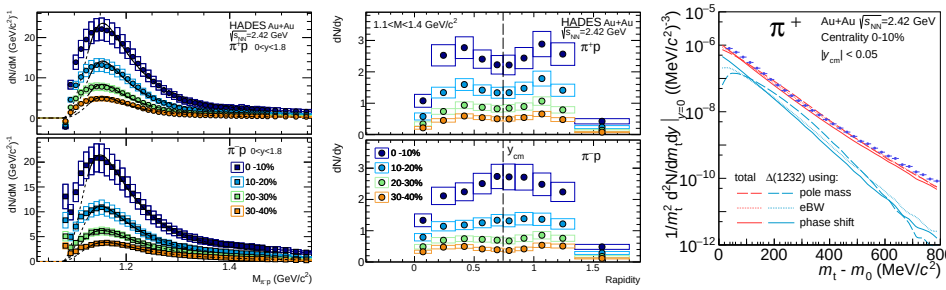

Fig. 6. Left: invariant mass distribution of correlated $\pi^- p$ and $\pi^+ p$ pairs, measured in Au+Au collisions at $\sqrt{s_{NN}} = 2.42$ GeV for different event centrality classes; middle: rapidity distributions of $\pi^+ p$ and $\pi^- p$ pairs in the same collisions; right: transverse mass distribution of π^+ overlaid with spectra calculated under different assumptions on the $\Delta(1232)$ shape (see the main text for details).

The importance of the proper resonance treatment is highlighted in the right panel of Fig. 6. The π^+ spectrum measured by HADES [7] is compared to spectra generated with the THERMINATOR 2 Monte Carlo generator [19, 20] using three different approaches. In the first approach, the only one available before, resonances always have their nominal mass. In the

second one, mass is sampled from the energy-dependent Breit–Wigner distribution. In the third approach, it is sampled from the distribution obtained as the derivative of the phase shift in the pion–proton scattering [21]. The last approach is the best in describing the slope of the experimental spectrum. This is especially important when the contribution from the $\Delta(1232)$ feed-down is large due to the relatively high freeze-out $T = 63.5$ MeV$/k_{\mathrm{B}}$, proposed in [22], which is used here.

7. Measurement of the hypernuclei lifetime

Production of hypernuclei, *i.e.* nuclear clusters containing hyperons instead of one (or more) nucleons, is driven both by strangeness production and cluster formation in heavy-ion collisions. HADES measures a number of them and contributes to the lifetime determination of ${}^{3}_{\Lambda}\mathrm{H}$, ${}^{4}_{\Lambda}\mathrm{H}$, as it is discussed in [10].

8. Outlook

HADES provides a wide range of observables measured with high statistical and systematic precision in heavy-ion collisions in the few-GeV energy regime. In this way, it reaches the region of largest μ_B in the QCD phase diagram of the currently running experiments. In the future, an excitation function of Au+Au collision energies (below the maximum of $\sqrt{s_{NN}} = 2.42$ GeV at SIS18) will be measured. Conditions in the produced medium will come closer to the vicinity of the critical point of the liquid-gas phase transition in the hadronic matter. This will allow to study the sensitivity of dilepton and fluctuation observables to the critical behavior of the medium.

Further inputs to the theoretical description of the strong interaction will be brought by the analysis of recently collected data on $p + p$ collisions at $\sqrt{s} = 3.46$ GeV. A $\pi^- p$ collision experiment with $\sqrt{s} \approx 2$ GeV is planned for the nearest future to access the third resonance region.

This work has been supported by SIP JUC Cracow, Poland, 2017/26/M/ST2/00600; TU Darmstadt, Germany, VH-NG-823, DFG GRK 2128, DFG CRC-TR 211, BMBF:05P18RDFC1; Goethe-University, Frankfurt, Germany and TU Darmstadt, Germany, ExtreMe Matter Institute EMMI at GSI Darmstadt; JLU Giessen, Germany, BMBF:05P12RGGHM; IPN Orsay, France, CNRS/IN2P3; NPI CAS, Řež, Řež, Czech Republic, MSMT LTT17003, MSMT LM2018112, MSMT OP VVV CZ.02.1.01/0.0/0.0/18_046/0016066.

REFERENCES

[1] HADES and PANDA collaborations (J. Adamczewski-Musch *et al.*), *Eur. Phys. J. A* **57**, 138 (2021), arXiv:2010.06961 [nucl-ex].

[2] HADES Collaboration (G. Agakishiev *et al.*), *Phys. Lett. B* **690**, 118 (2010), arXiv:0910.5875 [nucl-ex].

[3] HADES Collaboration (J. Adamczewski-Musch *et al.*), *Eur. Phys. J. A* **53**, 149 (2017), arXiv:1703.08575 [nucl-ex].

[4] HADES Collaboration (J. Adamczewski-Musch *et al.*), *Phys. Rev. C* **95**, 065205 (2017), arXiv:1703.07840 [nucl-ex].

[5] I. Frohlich *et al.*, *J. Phys.: Conf. Ser.* **219**, 032039 (2010), arXiv:0905.2568 [nucl-ex].

[6] HADES Collaboration (J.-H. Otto *et al.*), *Acta Phys. Pol. B Proc. Suppl.* **16**, 1-A131 (2023), this issue.

[7] HADES Collaboration (J. Adamczewski-Musch *et al.*), *Eur. Phys. J. A* **56**, 259 (2020), arXiv:2005.08774 [nucl-ex].

[8] HADES Collaboration (J. Adamczewski-Musch *et al.*), arXiv:2202.12750 [nucl-ex].

[9] HADES Collaboration (J. Adamczewski-Musch *et al.*), *Phys. Lett. B* **793**, 457 (2019), arXiv:1812.07304 [nucl-ex].

[10] HADES Collaboration (S. Spies *et al.*), *Acta Phys. Pol. B Proc. Suppl.* **16**, 1-A146 (2023), this issue.

[11] K. Fukushima, T. Kojo, W. Weise, *Phys. Rev. D* **102**, 096017 (2020), arXiv:2008.08436 [hep-ph].

[12] F. Seck *et al.*, *Phys. Rev. C* **106**, 014904 (2022), arXiv:2010.04614 [nucl-th].

[13] HADES Collaboration (R. Abou Yassine *et al.*), arXiv:2205.15914 [nucl-ex].

[14] M. Zétényi *et al.*, *Phys. Rev. C* **104**, 015201 (2021), arXiv:2012.07546 [nucl-th].

[15] G. Ramalho, M.T. Peña, *Phys. Rev. D* **95**, 014003 (2017), arXiv:1610.08788 [nucl-th].

[16] G. Ramalho, M.T. Peña, *Phys. Rev. D* **101**, 114008 (2020), arXiv:2003.04850 [hep-ph].

[17] G. Kornakov, T. Galatyuk, *Eur. Phys. J. A* **55**, 204 (2019), arXiv:1808.05466 [physics.data-an].

[18] HADES Collaboration (J. Adamczewski-Musch *et al.*), *Phys. Lett. B* **819**, 136421 (2021), arXiv:2012.01351 [nucl-ex].

[19] M. Chojnacki *et al.*, *Comput. Phys. Commun.* **183**, 746 (2012), arXiv:1102.0273 [nucl-th].

[20] S. Harabasz *et al.*, *Phys. Rev. C* **102**, 054903 (2020), arXiv:2003.12992 [nucl-th].

[21] P.M. Lo *et al.*, *Phys. Rev. C* **96**, 015207 (2017), arXiv:1703.00306 [nucl-th].

[22] A. Motornenko *et al.*, *Phys. Lett. B* **822**, 136703 (2021), arXiv:2104.06036 [hep-ph].